A Deterministic EM Design Technique for General Waveguide Dual-Mode Bandpass Filters

Hai Hu, *Student Member, IEEE*, and Ke-Li Wu, *Fellow, IEEE*

***Abstract*—Circular waveguide dual-mode (CWDM) filters have been widely employed in the manifold-coupled output multiplexer (OMUX) for satellite payloads. In this paper, a deterministic electromagnetic (EM) design technique for fast and accurately computerized prototyping a general CWDM filter is presented. By introducing a generalized K impedance inverter using the generalized scattering matrix of the tuning screw section, the insertion phase and the coupling of the two degenerate modes in a CWDM cavity can be determined by a most effective way. To handle the asynchronously tuned cases, the theoretical formula that relates a self-coupling to its corresponding phase offset is derived. The design technique is based on modal analysis at the center frequency and is deterministic without using optimization or curve fitting. The presented technique enables the full-wave EM design of CWDM filters as easy and accurate as designing conventional single mode waveguide filters. To validate the design technique, practical design of eight-pole symmetric and asymmetric CWDM filters have been studied theoretically and experimentally. An EM design of a complete Ku-band 15-channel contiguous OMUX is also demonstrated.**

***Index Terms*—Dual-mode waveguide filter.**

I. Introduction

CIRCULAR waveguide dual-mode (CWDM) filters are widely used as channel filters in output multiplexers (OMUXs) of a communication satellite payload system due to its compact size, high unloaded Q, and flexibility in realizing various required cross couplings [1], [2]. Since its birth at ComSat Laboratories 40 years ago in response to very stringent performance requirements upon spacecraft microwave equipment, the CWDM filter has been a vital workhorse for the OMUXs in Ku and Ka frequency bands. Since there are too many variables to tune in designing a complete OMUX as one unit, an effective methodology for designing an OMUX with a high number of channels consists of: 1) synthesizing the OMUX circuit model (which include the coupling matrices of channel filters, manifold, and stub lengths) that meets the required channel rejections and common port return loss (CPRL); 2) designing physical dimensions of each segregated channel filter using an EM simulation tool according to the synthesized circuit model; and 3) assembling all the electromagnetic (EM) models of designed channel filters to the waveguide manifold for fine adjustments [3]–[5]. Due to the complex load effect [6], each channel filter when detached from the manifold, is an asynchronously tuned filter. In general, a Chebyshev filter with asymmetric filtering characteristic is an asynchronously tuned filter [7]. Therefore, it will be of great benefit to the microwave industry to develop an efficient technique that automatically designs an accurate physical model of a general CWDM filter. A good design technique should be deterministic (without optimization or curve-fitting), efficient, and versatile.

An accurately designed physical model of a CWDM filter is highly desirable by the industry in three aspects, which are: 1) to provide precise physical dimensions of channel filters that share the same circuit models as those used for computer-aided tuning (CAT) [8]; 2) to accurately predict the spurious mode behavior for design assurance; and 3) to perform necessary auxiliary analysis, such as thermal analysis and multipaction analysis [9], [10] for estimating high power-handling capability. Any of these tasks would be impossible without an effective EM design technique in the first place. An efficient design technique enables rapid EM prototyping of an OMUX with a large number of channel filters so that designers are capable of conducting design tradeoff in a short design cycle.

The most challenging issue in EM design of a CWDM filter is design of tuning and coupling elements in a dual-mode cavity for adjusting the resonance frequency offsets and the coupling between the two orthogonal degenerate modes, namely, TE_{11v} and TE_{11h}, which are denoted as v and h modes, respectively, in this paper. In practice, the most commonly used tuning and coupling structures are metal tuning screws. Although many alternative dual-mode cavity structures are proposed in the past decades for facilitating full-wave EM modeling [11]–[14], this paper will focus on the traditional CWDM filter with a square cross-section screw model representing the actual round tuning screw. Nevertheless, the proposed theory is generic and applicable to all the other narrowband (factional bandwidth $<2\%$) waveguide dual-mode cavity configurations.

By a traditional EM design technique, the coupling coefficient of two degenerate modes can be determined by the frequency difference of two eigenmodes in a short-ended synchronously tuned CWDM cavity [11]–[13], [15]–[18]. The parameter is obtained either by frequency sweeping of S-parameters or by solving an eigenvalue problem. A simple inverter model that imitates the coupling of two degenerate modes in a short-ended dual-mode cavity was proposed in [14], which allows an approximate calculation of the coupling coefficient using the generalized scattering matrix (GSM) of the tuning and

Manuscript received June 14, 2012; revised November 18, 2012; accepted November 20, 2012. Date of publication December 20, 2012; date of current version February 01, 2013. This work was supported by the University Grants Committee of the Hong Kong Special Administrative Region under Grant AoE/P-04/08.

The authors are with the Department of Electronic Engineering, The Chinese University of Hong Kong, Shatin, NT, Hong Kong (e-mail: hhu@ee.cuhk.edu.hk; klwu@ee.cuhk.edu.hk).

Color versions of one or more of the figures in this paper are available online at http://ieeexplore.ieee.org.

Digital Object Identifier 10.1109/TMTT.2012.2231874

coupling section when coupling is weak. Nevertheless, none of the existing approaches has addressed the fundamental relationship between the v and h modes, frequency offsets specified by the corresponding self-couplings, and the length of related CWDM cavity. These fundamental issues are critical especially when the filter order is high and insertions of the tuning screws are reasonably large in a CWDM cavity.

This paper will give effective answers to all these issues. The proposed technique will systematically determine all the required physical parameters associated to the coupling matrix of a CWDM filter, which possesses a general Chebyshev filtering characteristic with appropriate coupling topology realizable for CWDM filters. Although some preliminary result of this technique was briefly reported in [19], the detailed development of the design theory for modeling the coupling between the v and h modes in a deterministic manner, as well as the frequency-offset of each degenerate mode will be given in this paper. With the proposed theory, a complete CWDM filter can be automatically designed deterministically by full-wave EM modal analysis only at filter center frequency.

The versatility, efficiency, and accuracy of the proposed design technique are demonstrated by three full-wave EM design examples, including an eight-pole CWDM filter with hardware test prototype for experiment verification, a Ku-band eight-pole filter in asymmetric box configuration, and a complete Ku-band 15-channel contiguous OMUX.

II. Design Theory

A waveguide dual-mode filter is usually realized in cascade-quartet (CQ) or in-line coupling topology [20]. It works only when two conditions are satisfied, which are: 1) all the coupling elements, such as irises and tuning screws, provide the correct amount of couplings and 2) degenerate modes in a CWDM cavity resonate at the correct frequencies, for which all the resonance phase contributions by irises and the tuning screws must be taken into account. It will be shown that the two conditions will be satisfied in the design process by employing the GSM at the center frequency of the filter.

A. Self-Coupling Effect

The self-coupling coefficient, or the frequency-invariant reactance (FIR) in the filter low-pass circuit model, quantifies the frequency offset of each electric resonator. It must be considered in designing an asynchronously tuned CWDM filter.

For an asynchronously tuned bandpass filter prototype network [20], if the resonance frequency is shifted by Δf in the ith resonator, the normalized impedance of the loop equations obtained using KCL can be found to be

$$z_{ii} = \frac{f_0}{\mathrm{BW}}\left(\frac{f}{f_0+\Delta f} - \frac{f_0+\Delta f}{f}\right) \tag{1}$$

which can be well approximated when $\Delta f \ll f_0$ by

$$z_{ii} \approx \frac{f_0}{\mathrm{BW}}\left(\frac{f}{f_0} - \frac{f_0}{f}\right) - 2\frac{\Delta f}{\mathrm{BW}} \tag{2}$$

where f is frequency, Δf is the resonance frequency shift from the center frequency f_0 of the filter, and BW is the filter bandwidth. According to the loop equation formulated using the coupling matrix, the first term in (2) is the frequency variable in the low-pass filter prototype, while the second term contributes to the ith diagonal term of the coupling matrix, and is called self-coupling

$$M_{ii} = -2\frac{\Delta f}{\mathrm{BW}}. \tag{3}$$

In a general waveguide, the phase constant β for the operating mode (such as TE_{11} for a cylindrical cavity) is given by

$$\beta = \sqrt{k^2 - k_c^2} \tag{4}$$

where k is the free-space wavenumber and k_c is the waveguide cutoff wavenumber. At f_0, the slope of β with respect to f can be found by

$$S_0 = \left.\frac{d\beta}{df}\right|_{f=f_0} = \left(\frac{2\pi}{c}\right)^2 \frac{f_0}{\beta_0} = \frac{\lambda_{g0}}{\lambda_0}\frac{2\pi}{c} \tag{5}$$

where β_0, λ_0 and λ_{g0} are the phase constant, free-space wavelength, and waveguide wavelength at f_0, respectively.

In the vicinity of f_0, the frequency change Δf due to the self-coupling in (3) can then be related to an incremental change in phase constant $\Delta\beta$ through S_0. If the cavity length is l_0, whose electrical length is $k_n\pi$ (k_n is an integer), a small phase change $\Delta\varphi$ caused by Δf can be found as

$$\Delta\varphi = l_0 S_0 \Delta f = \left(\frac{\lambda_{g0}}{\lambda_0}\right)^2 \frac{\Delta f}{f_0} k_n\pi. \tag{6}$$

Substituting (3) into (6), the phase change contributed by a self-coupling can be revealed by

$$\Delta\varphi = -\left(\frac{\lambda_{g0}}{\lambda_0}\right)^2 \frac{\mathrm{BW}}{f_0}\frac{M_{ii}}{2} k_n\pi. \tag{7}$$

B. Generalized K Inverter for Screw Section Design

Considering a three tuning screw section placed in a maximum electric field location in longitudinal direction of a $k_n\pi$-long dual-mode cavity, as illustrated in Fig. 1(a), in which k_n is assumed to be an odd number, t_h, t_v, and t_f are penetration depths for the screws inserted at 0°, 90°, and 225° (45°, −45°, or 135°), respectively. This section provides the required coupling between the v and h modes and creates insertion phases φ_{vM} and φ_{hM} for achieving necessary phase balance in a CWDM cavity.

A multiport network based on the GSM of the three tuning screws section at the center frequency is used to describe the interaction of the relevant modes. To represent the coupling of the v and h modes, all the modes considered in the GSM need to be short circuited at both ends of the cavity with electric lengths of $(k_n\pi/2 - \varphi_{vM}/2)$ and $(k_n\pi/2 - \varphi_{hM}/2)$, except for the dominant v and h modes. Having short circuited the higher order modes in the multiport network, an ordinary two-port network is created, which is illustrated in Fig. 1(b). By physical intuition, it is known that the electrical lengths of the two short-circuited stubs correspond to the resonant lengths of the two degenerate modes at center frequency. By specifying the h mode

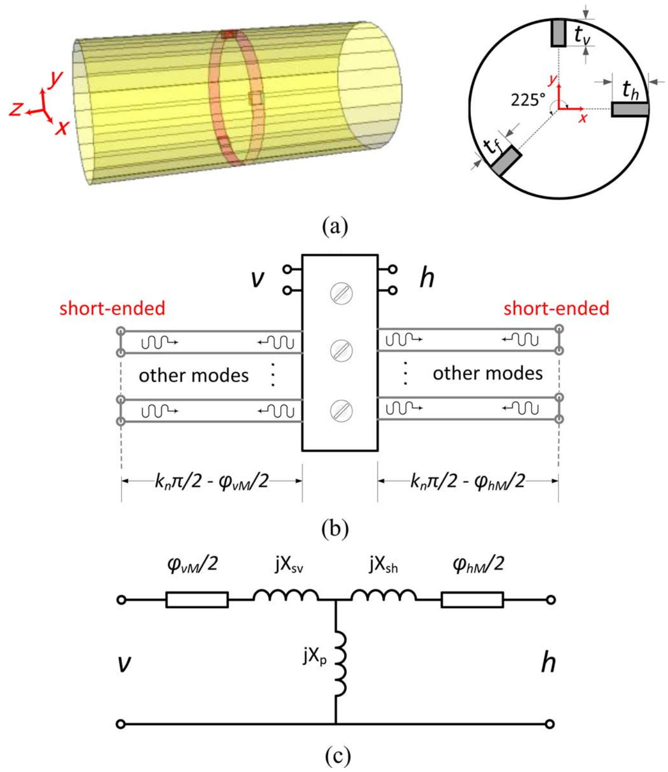

Fig. 1. Tuning and coupling screws section in a CWDM cavity. (a) Physical structure. (b) Generalized K inverter model in terms of GSM. (c) Equivalent circuit of the K inverter model.

at one matched port and the v mode at the other matched port, a generalized inverter K can be introduced, which represents the interactions between all the modes in the cavity. Since the phase contributions to the v and h modes by the irises at the ends of the cavity and the required self-coupling of the v and h mode are different, the electrical lengths of the two short-circuited stubs in the K inverter are different. In other words, the resultant two-port network is asymmetric in general. The equivalent circuit of the K inverter model shown in Fig. 1(c) serves as the basic circuit model for determining the coupling of the two degenerate modes, as well as the insertion phases introduced by the tuning section. The parameters in the circuit model can be found in terms of the S-parameters of the K inverter model sketched in Fig. 1(b) as

$$
\begin{aligned}
jX_p &= \frac{2S_{21vh}}{(1-S_{11vv})(1-S_{22hh})-S_{21vh}^2} \\
jX_{sv} &= \frac{(1+S_{11vv})(1-S_{22hh})+S_{21vh}^2-2S_{21vh}}{(1-S_{11vv})(1-S_{22hh})-S_{21vh}^2} \\
jX_{sh} &= \frac{(1-S_{11vv})(1+S_{22hh})+S_{21vh}^2-2S_{21vh}}{(1-S_{11vv})(1-S_{22hh})-S_{21vh}^2}
\end{aligned} \tag{8}
$$

from which the inverter K, as well as the insertion phases φ_{vM} and φ_{hM} can then be derived and are given by (9) and (10), shown at the bottom of this page, where

$$
\begin{aligned}
a &= 1 + X_{sv}/X_p \\
b &= j(X_{sv} + X_{sh} + X_{sv}X_{sh}/X_p) \\
c &= 1/jX_p \\
d &= 1 + X_{sh}/X_p \\
\alpha &= \tan^{-1}[j(a+d)/(c+b)] \\
\beta &= \tan^{-1}[j(a-d)/(c-b)].
\end{aligned}
$$

The above equations are subject to the scattering parameters that are normalized to the matched loads at the two ports. The derivation and other applications of a generalized K inverter model can also be found in [21].

It can be shown that the coupling M of the two degenerate modes is scaled to the impedance inverter K by [22]

$$K = \left(\frac{\lambda_{g0}}{\lambda_0}\right)^2 \frac{\mathrm{BW}}{f_0}\frac{M}{2} k_n \pi \tag{11}$$

where $\lambda_0$is free-space wavelength and λ_{g0} is the waveguide wavelength at f_0.

It is worth mentioning that a simple circuit model based on an impedance inverter was proposed in [14] for determining M, φ_{vM} and φ_{hM}. However, the model is inadequate in three aspects, which are: 1) only the fundamental mode is considered in the two short-circuited stubs, meaning that the interactions between the reflected higher order modes and the cavity end walls are ignored; 2) only the special case where the K inverter circuit model is symmetric has been considered; and 3) the insertion phase φ_{vM} and φ_{hM} are approximated by the phase of S_{12} of the three tuning screws section rather than rigorously determined from the K inverter circuit model. These limitations have restricted the use of the circuit model proposed in [14] only to the design of synchronously tuned CWDM filters with very small fractional bandwidth in which screw penetration is small and the approximated insertion phases is acceptable.

The screw penetration depths t_f, t_v, and t_h that provide the required M, φ_{vM} and φ_{hM} can then be found by following the flowchart shown in Fig. 2, where the bisection method is used to determine the dimension variables one at a time. Since the coupling value and the insertion phases can be found by the generalized K impedance inverter with the GSM of the section at f_0, the design process can be remarkably fast.

C. Automatic Design Procedure

The input/output coupling and the inter-cavity coupling can be calculated directly by the conventional K impedance inverter [12], [16] model with respect to the fundamental mode because

$$K = \sqrt{\frac{(b+c)\cos\alpha + (b-c)\cos\beta + j(a+d)\sin\alpha - j(a-d)\sin\beta}{(b+c)\cos\alpha - (b-c)\cos\beta + j(a+d)\sin\alpha + j(a-d)\sin\beta}} \tag{9}$$

$$
\begin{aligned}
\varphi_{vM} &= (\alpha+\beta)/2 \\
\varphi_{hM} &= (\alpha-\beta)/2
\end{aligned} \tag{10}
$$

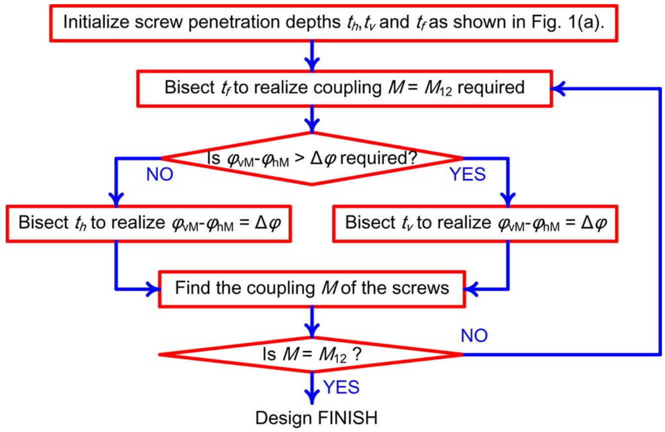

Fig. 2. Design flowchart of the screw section where M_{12} is the required degenerate mode coupling and $\Delta\varphi$ is the required phase difference between the v and h modes.

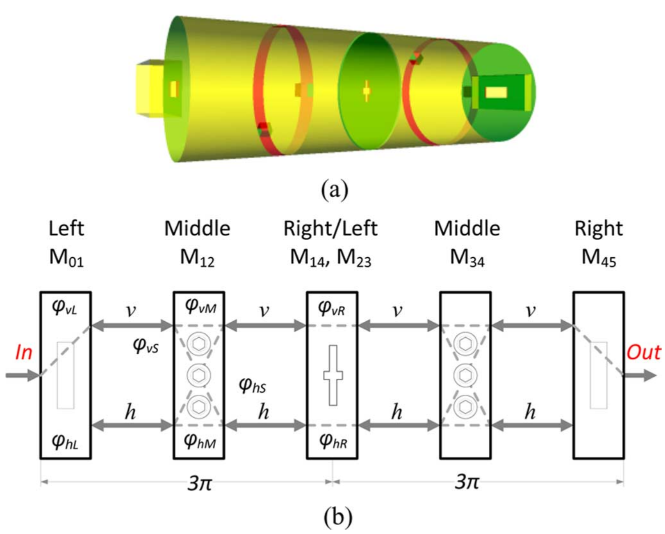

Fig. 3. Typical fourth-order CWDM filter. (a) Physical structure. (b) Building block diagram.

the calculation only involves the coupling of two single modes in two separately matched waveguides [14], [15], [22]. Together with the generalized K impedance inverter for modeling the tuning screw section, an automatic EM design procedure for a CWDM cavity filter can then be established.

The procedure can guide the design of a CWDM filter of any order. Consider a typical fourth-order 3π-long CWDM filter as an example: the physical structure of the filter, as depicted in Fig. 3(a), is decomposed into five basic coupling blocks, which are cascaded at their circular waveguide interfaces, as shown in Fig. 3(b). The design procedure goes cavity by cavity and coupling element by coupling element from left to right. Each designed coupling element contributes to both the coupling value and the insertion phase of the two degenerate modes.

In the design process, phase shifts due to the nonzero self-coupling M_{11} and M_{22} are firstly determined by (7). The M_{01} and M_{14}/M_{23} coupling blocks in the first cavity are then designed to realize the corresponding couplings, followed by the design of the middle M_{12} coupling block to realize the required coupling between the two degenerate modes in the first CWDM cavity and to balance the phase loadings of the v and h modes in the same cavity according to the phase balance condition in a CWDM cavity

$$\varphi_{vL} + \varphi_{vM} + \varphi_{vR} + \varphi_{vS} = \varphi_{hL} + \varphi_{hM} + \varphi_{hR} + \varphi_{hS} \quad (12)$$

which is equal to $\Delta\varphi_T$, the total phase change from end to end in the CWDM cavity. On the left-hand side of (12), $\varphi_{vL}, \varphi_{vM}, \varphi_{vR}$, and φ_{vS} are the phase shifts caused by the coupling elements for M_{01}, M_{12}, M_{14}/M_{23} and M_{11}, respectively, all for the v mode. Similar definitions for the h mode apply to the right-hand side of (12) with M_{11} replaced by M_{22}. The cavity waveguide lengths on the both sides of the three tuning screw section are then determined by $(3\pi - \Delta\varphi_T)/(2\beta_0)$. Having had every coupling element in each cavity successively designed, all the designed cavities will be cascaded to create the final EM model of the CWDM filter.

TABLE I
COUPLING MATRIX FOR THE EIGHT-POLE CWDM FILTER

M_{01}	1.0090	M_{34}	0.5014	M_{67}	0.4348
M_{12}	0.7991	M_{45}	0.5526	M_{78}	0.8024
M_{14}	-0.2466	M_{56}	0.5559	M_{89}	1.0090
M_{23}	0.7533	M_{58}	0.2358		

III. DESIGN EXAMPLES

To demonstrate the accuracy and efficiency of the developed theory, a fully automatic design tool has been developed, which drives the full-wave commercial EM modal analysis software μWave Wizard [23], for full-wave EM design of a general CWDM filter. Two practical individual CWDM filters and one OMUX are investigated in this paper, including experimental verification by a Ku-band eight-pole CWDM bandpass filter. The designed EM responses are compared with those of the counterpart coupled resonator circuit models, showing excellent agreement.

Design Example 1: Ku-Band Eight-Pole CWDM Filter: An eight-pole Ku-band synchronously tuned filter is firstly EM designed using the proposed design technique. The filter to be designed has $f_0 = 12.445$ GHz, BW $= 55$ MHz, and the required coupling matrix is given in Table I. The filter is realized by four 3π electrical-long CWDM cavities with $R = 13.0$ mm and WR75 rectangular waveguide at the input and output ports. The thickness of each coupling iris is 0.5 mm and the square tuning screw cross section is 3.0×3.0 mm^2. The whole automatic design process takes 11 min with more than 900 modes considered in the modal analysis of each discontinuity. A hardware filter is built with the designed filter dimensions and is fine tuned according to the required coupling matrix using a computer-aided tuning technology [8].

The obtained in-band responses from the synthesized circuit model, the full-wave EM model, and the measurement are superimposed in Fig. 4(a). It can be seen the designed EM model provides an accurate filter hardware design that matches the required circuit model. For reader's information, in this example, the cutoff frequencies of the highest mode for calculating each junction and connecting the junctions are 130 and 15 GHz, respectively. The 2-D FEM mesh size is 0.6142 mm for all irises and screw sections. Furthermore, as shown in Fig. 4(b), in which

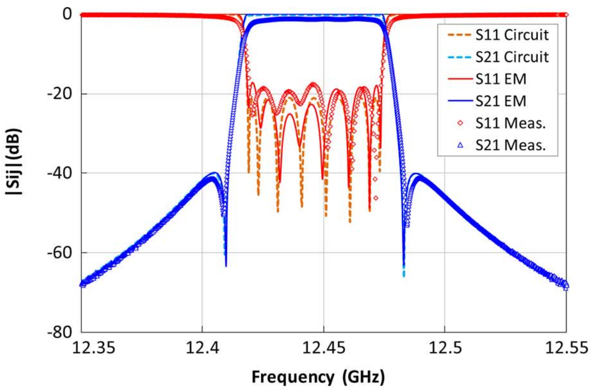

(a)

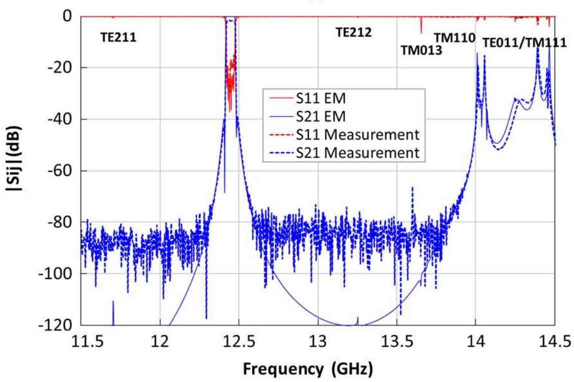

(b)

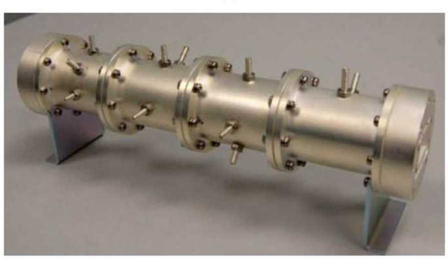

(c)

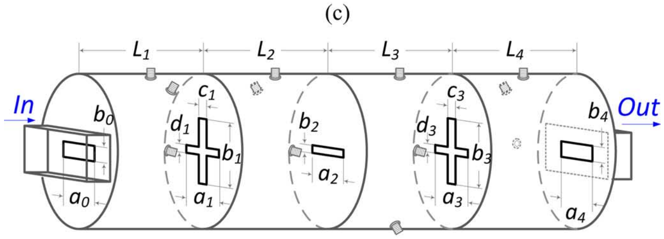

(d)

Fig. 4. Physical model of the designed eight-pole CWDM filter. (a) In-band and (b) broadband S-parameter responses. (c) Photograph of the manufactured filter hardware. (d) Filter geometry parameters illustration.

broadband responses from both the full-wave EM model and the measurement are superimposed, the EM designed model can well predict the spurious mode behavior. The manufactured filter hardware is shown in Fig. 4(c), and the dimensions of the designed EM model and those measured from the finally tuned hardware filter are compared in Table II with the geometry parameters illustrated in Fig. 4(d). The noticeable deviations of the hardware's L_2 and L_3 from those of the EM model are caused by a known large manufacturing error. Nevertheless, these deviations can be compensated by the tuning screws.

TABLE II
DIMENSION COMPARISON BETWEEN THE EM AND HARDWARE MODEL OF THE EIGHT-POLE CWDM FILTER IN DESIGN EXAMPLE 1 (UNIT: MILLIMETERS)

	EM Model	Hardware		EM Model	Hardware
a_0	8.787	8.64	b_4	1.900	1.91
a_1	4.547	4.33	c_1	1.500	1.51
a_2	5.745	5.34	c_3	1.500	1.53
a_3	4.468	4.25	d_1	1.500	1.52
a_4	8.787	8.63	d_3	1.500	1.51
b_0	1.900	1.91	L_1	42.452	42.35
b_1	6.311	6.16	L_2	42.861	42.16
b_2	1.509	1.50	L_3	42.867	42.18
b_3	5.423	5.20	L_4	42.456	42.38

TABLE III
SCREW PENETRATIONS IN EACH CAVITY OF THE EIGHT-POLE CWDM FILTER IN DESIGN EXAMPLE 1 (UNIT: MILLIMETERS)

screws in cavity 1	t_f 45°=	1.7998	*screws in cavity 3*	t_f -45°=	1.4235
	t_h 0°=	2.5406		t_h 0°=	1.0102
	t_v 90°=	0.6000		t_v 90°=	0.6000
screws in cavity 2	t_f 135°=	1.3227	*screws in cavity 4*	t_f 135°=	1.8157
	t_h 0°=	0.6234		t_h 180°=	2.6437
	t_v 90°=	0.6000		t_v 90°=	0.6000
screw cross section = 3.0×3.0 mm^2					

TABLE IV
PHASE CONTRIBUTION FROM EACH ELEMENT IN THE CWDM CAVITIES OF DESIGN EXAMPLE 1 (UNIT: DEGREES)

	φ_{vL}	φ_{vR}	φ_{vM}	φ_{vS}	φ_{hL}	φ_{hR}	φ_{hM}	φ_{hS}
cav1	6.35	0.58	37.91	0	0.29	1.44	43.11	0
cav2	0.58	1.02	38.11	0	1.44	0.12	38.15	0
cav3	1.02	0.54	38.05	0	0.12	0.88	38.62	0
cav4	0.54	6.35	37.90	0	0.88	0.29	43.62	0

The designed screw penetrations are listed in Table III, where the screw types (t_f followed by a penetration angle indicates the coupling screw, t_h and t_v indicate the h and v mode tuning screws, respectively) are also marked. Generally speaking, only two screws needs to be adjusted in each cavity to realize required coupling and phase balance; a third screw with a preset penetration is for providing any possible two-direction tuning to compensate any manufacture tolerance without changing the cavity length. In Table III, $t_v 90^\circ$ is set to be 0.6 mm.

The v and h mode phase shifts contributed by the finally realized irises and screws in each cavity are listed in Table IV, where it can be seen they meet the phase balance condition (12).

Design Example 2: Ku-band Eight-Pole Filter in Asymmetric Box Coupling Configuration: In this example, an eight-pole CWDM filter realizing box coupling topology [20], as sketched in Fig. 5, is full-wave EM designed. The filter is capable of providing two asymmetric transmission zeroes. The filter with such rejection characteristic must be asynchronously tuned.

The eight-pole filter has $f_0 = 12.0$ GHz, $\mathrm{BW} = 50$ MHz, and its coupling matrix is given in Table V, which will generate two transmission zeroes on the upper rejection band. The filter is realized by four 3π electrical-long CWDM cavities with $R = 13.5$ mm and WR75 rectangular waveguide at the input and output ports. The physical model of the filter is illustrated in Fig. 6. The first cruciform iris realizes M_{13} and M_{24} as electrical resonators 1 and 3 are two v modes, while resonators 2 and 4 are

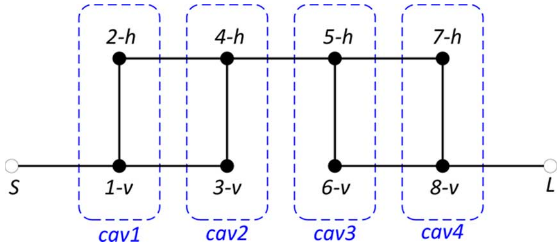

Fig. 5. Coupling schematic of the eight-pole box coupling configuration to be realized by a CWDM filter, each dashed box represents a CWDM cavity.

TABLE V
COUPLING MATRIX FOR THE EIGHT-POLE CWDM FILTER IN BOX TOPOLOGY

M_{01}	1.0483	M_{57}	-0.2528	M_{44}	0.0615
M_{12}	0.4134	M_{68}	0.7433	M_{55}	0.0592
M_{13}	0.7680	M_{78}	0.4563	M_{66}	0.3467
M_{24}	-0.2153	M_{89}	1.0483	M_{77}	-0.8438
M_{34}	0.5223	M_{11}	0.0184	M_{88}	0.0184
M_{45}	0.5515	M_{22}	-0.8924		
M_{56}	0.5032	M_{33}	0.2854		

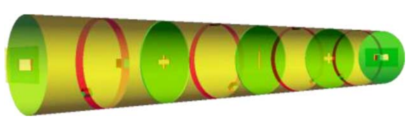

Fig. 6. Physical structure of the eight-pole CWDM filter in a box coupling topology.

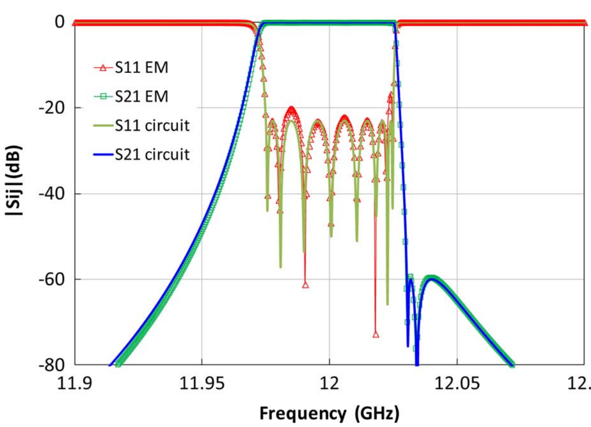

Fig. 7. S-parameters of the full-wave EM model and the circuit model of the eight-pole CWDM filter in a box coupling topology.

TABLE VI
EM DESIGNED IRISES AND CAVITY DIMENSIONS OF THE EIGHT-POLE CWDM FILTER IN A BOX COUPLING TOPOLOGY (UNIT: MILLIMETERS)

a_0	8.647	b_1	4.427	d_1	1.500
a_1	6.485	b_2	6.251	d_3	1.500
a_2	1.000	b_3	4.674	L_1	41.497
a_3	6.457	b_3	3.000	L_2	41.966
a_4	8.647	c_1	1.500	L_3	41.967
b_0	3.000	c_3	1.500	L_4	41.496

two h modes in the first two CWDM cavities. Similar geometric arrangement applies to the other two cavities. The M_{45} coupling structure in between the second and third CWDM cavities now must be a vertical slot so as to couple two h modes.

TABLE VII
SCREW PENETRATIONS IN EACH CAVITY OF THE EIGHT-POLE CWDM FILTER IN BOX COUPLING TOPOLOGY (UNIT: MILLIMETERS)

screws in cavity 1	t_f 225°=	1.4397	screws in cavity 3	t_f -45°=	1.6117
	t_h 0°=	2.8175		t_h 0°=	0.2000
	t_v 90°=	0.2000		t_v 90°=	0.9757
screws in cavity 2	t_f -45°=	1.6402	screws in cavity 4	t_f 225°=	1.5293
	t_h 0°=	0.2000		t_h 0°=	2.8154
	t_v 90°=	0.7687		t_v 90°=	0.2000
screw cross section = 2.5×2.5 mm^2					

TABLE VIII
PHASE CONTRIBUTION FROM EACH ELEMENT IN THE CWDM CAVITIES OF DESIGN EXAMPLE 2 (UNIT: DEGREES)

	φ_{vL}	φ_{vR}	φ_{vM}	φ_{vS}	φ_{hL}	φ_{hR}	φ_{hM}	φ_{hS}
cav1	6.32	1.37	29.92	-0.03	0.63	0.49	35.05	1.42
cav2	1.37	0.00	31.01	-0.46	0.49	0.94	30.59	-0.10
cav3	0.00	1.34	31.12	-0.55	0.94	0.55	30.51	-0.09
cav4	1.34	6.32	29.97	-0.03	0.55	0.63	35.07	1.35

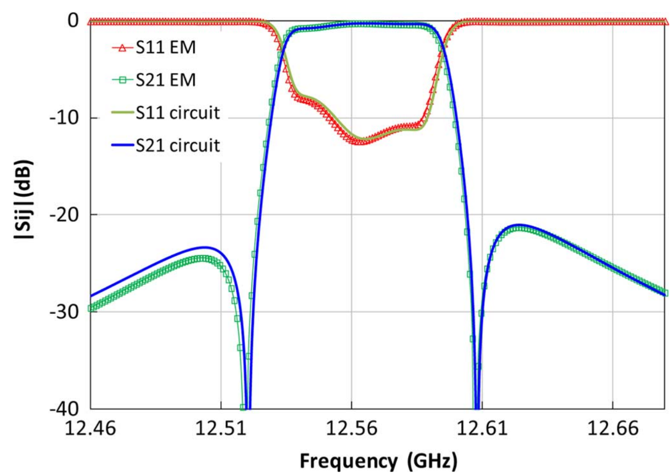

Fig. 8. S-parameters of the full-wave EM model and the circuit model of the 15th channel CWDM filter of a Ku-band 15-channel OMUX.

The presented design theory and procedure can be applied to this design requirement in a straightforward manner. The total EM design time is about 11 min with more than 900 modes considered for modal analysis of each coupling structure. The obtained full-wave EM designed responses and those of the target coupling matrix are given in Fig. 7, showing excellent agreement.

The iris dimensions and cavity lengths of the designed EM model are listed in Table VI, where the geometry parameters illustration can be found in Fig. 4(d). The tuning screw penetration depths for each CWDM cavity are listed in Table VII. The v and h mode phase shifts contributed by the designed irises and screws are listed in Table VIII.

Design Example 3: Ku-band 15-Channel Contiguous OMUX: A Ku-band 15-channel contiguous OMUX with included bandwidth of 900 MHz is full-wave EM prototyped in this example using the proposed design process. The center frequencies of the 15 channels are from 11.725 to 12.565 GHz, with 60-MHz bandwidth for each channel. The circuit model, which gives 22-dB CPRL for the OMUX, is first synthesized by the method introduced in [3]. The manifold is realized by

TABLE IX
COUPLING MATRIX FOR 15-CHANNEL FOUR-POLE CWDM FILTER

M_{01}	1.1224	M_{34}	0.8969	M_{33}	0.0510
M_{12}	0.6791	M_{45}	1.1104	M_{44}	0.0552
M_{14}	-0.2670	M_{11}	-0.3339		
M_{23}	0.7894	M_{22}	0.0379		

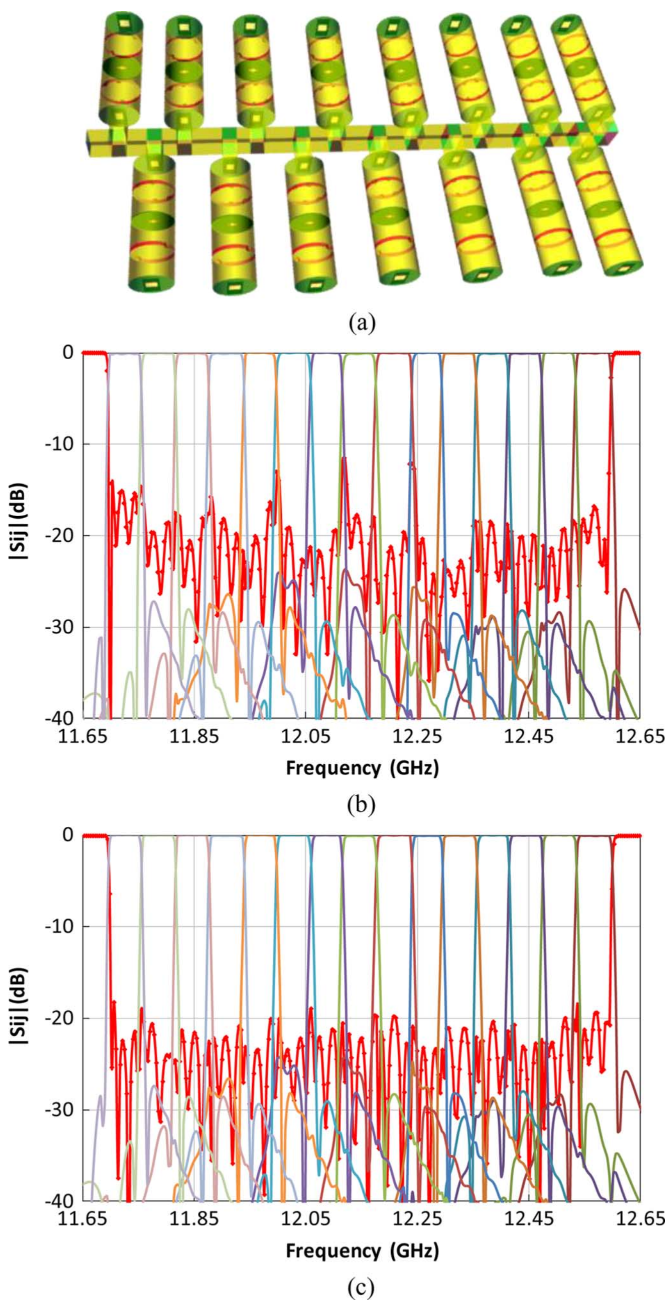

Fig. 9. Ku-band 15-channel contiguous OMUX. (a) Physical structure and S-parameter responses from: (b) the designed full-wave EM model and (c) the full-wave EM model with minor tuning.

WR75 rectangular waveguides connected by E-plane T-junctions. Each channel filter will be realized by a four-pole CWDM filter arranged in in-line coupling topology. The CWDM filter radius is chosen to be $R = 13.15$ mm and the operating mode is TE_{113}.

Considering the highest channel, channel 15, as an example, its coupling matrix is shown in Table IX, $f_0 = 12.5655$ GHz, and $\mathrm{BW} = 56.5$ MHz. The full-wave EM design time for the channel filter is less than 6 min with more than 900 modes considered in modal analysis. The responses from the resultant EM model for the channel filter and those from the targeted coupling matrix are compared in Fig. 8. It can be seen that the designed circuit model can be fully replaced by the EM model.

The other 14 channel filters can be full-wave designed one by one based on the design theory and procedure presented in this paper. After removing the phase-loading for each channel filter [8], all the 15-channel filters are assembled to the EM model of the manifold, as shown in Fig. 9(a). The responses of the whole OMUX is then quickly obtained by cascading the GSM of each channel filter with that of the manifold, and are shown in Fig. 9(b). It can be seen that without any optimization, the CPRL of the designed EM model of the specified OMUX already reaches a 20-dB level for most of channels. With minor tuning to the manifold stubs length alone, the OMUX in-band CPRL is easily pushed down below 20 dB contiguously, as shown in Fig. 9(c).

IV. CONCLUSION

An efficient and deterministic EM design technique of a general waveguide dual-mode filter has been presented. The design theory is developed by introducing a generalized K inverter model for describing the interaction of the two degenerate modes and other higher order modes in a CWDM cavity, with which the design procedure only requires full-wave EM modal analysis at the center frequency of the filter. The design process is very straightforward and is general to any waveguide dual-mode filter arranged in propagating coupling configuration. An automatic design software interfaced to a commercial EM modal analysis solver is developed for preparing the representative, practical and industrially challenging design examples presented in this paper, which include doubly and singly terminated, symmetric and asymmetric characteristics, and synchronously and asynchronously tuned CWDM filters. A design example of a complete Ku-band 15-channel OMUX are also presented to validate the proposed design technique. It can be concluded that the proposed design technique can provide the space microwave industry with an efficient design tool for advanced waveguide dual-mode filters.

REFERENCES

[1] A. E. Atia and A. E. Williams, "New types of waveguide bandpass filters for satellite transponders," *Comsat Tech. Rev.*, vol. 1, no. 1, pp. 21–43, Fall, 1971.

[2] A. E. Atia and A. E. Williams, "Narrow-bandpass waveguide filters," *IEEE Trans. Microw. Theory Techn.*, vol. MTT-20, no. 4, pp. 258–265, Apr. 1972.

[3] R. J. Cameron and M. Yu, "Design of manifold-coupled multiplexers," *IEEE Microw. Mag.*, vol. 8, no. 5, pp. 46–59, Oct. 2007.

[4] C. Kudsia, R. Cameron, and W.-C. Tang, "Innovations in microwave filters and multiplexing networks for communications satellite systems," *IEEE Trans. Microw. Theory Techn.*, vol. 40, no. 6, pp. 1133–1149, Jun. 1992.

[5] M. Yu and Y. Wang, "Synthesis and beyond," *IEEE Microw. Mag.*, vol. 12, no. 6, pp. 62–76, Oct. 2011.

[6] K.-L. Wu and W. Meng, “A direct synthesis approach for microwave filters with a complex load and its application to direct diplexer design,” *IEEE Trans. Microw. Theory Techn.*, vol. 55, no. 5, pp. 1010–1017, May 2007.
[7] D. S. G. Chambers and J. D. Rhodes, “A low-pass prototype network allowing the placing of integrated poles at real frequencies,” *IEEE Trans. Microw. Theory Tech.*, vol. MTT-31, no. 1, pp. 40–45, Jan. 1983.
[8] M. Meng and K.-L. Wu, “An analytical approach to computer-aided diagnosis and tuning of lossy microwave coupled resonator filters,” *IEEE Trans. Microw. Theory Techn.*, vol. 57, no. 12, pp. 3188–3195, Dec. 2009.
[9] J. Monge, J. Ruiz-Cruz, S. Anza, C. Vicente, K. Zaki, J. Montejo-Garai, J. Rebollar, J. Gil, B. Gimeno, and V. Boria, “High power analysis and design of dual-mode channel filters,” in *IEEE MTT-S Int. Microw. Symp. Dig.*, 2009, pp. 1353–1356.
[10] S. Anza, C. Vicente, D. Raboso, J. Gil, B. Gimeno, and V. Boria, “Enhanced prediction of multipaction breakdown in passive waveguide components including space charge effects,” in *IEEE MTT-S Int. Microw. Symp. Dig.*, 2008, pp. 1095–1098.
[11] X.-P. Liang, K. A. Zaki, and A. E. Atia, “Dual mode coupling by square corner cut in resonators and filters,” *IEEE Trans. Microw. Theory Techn.*, vol. 40, no. 12, pp. 2294–2302, Dec. 1992.
[12] J.-F. Liang, X.-P. Liang, K. A. Zaki, and A. E. Atia, “Dual-mode dielectric or air-filled rectangular waveguide filters,” *IEEE Trans. Microw. Theory Techn.*, vol. 42, no. 7, pp. 1330–1336, Jul. 1994.
[13] L. Accatino, G. Bertin, and M. Mongiardo, “A four-pole dual mode elliptic filter realized in circular cavity without screws,” *IEEE Trans. Microw. Theory Techn.*, vol. 44, no. 12, pp. 2680–2687, Dec. 1996.
[14] K.-L. Wu, “An optimal circular waveguide dual-mode filter without tuning screws,” *IEEE Trans. Microw. Theory Techn.*, vol. 47, no. 3, pp. 271–276, Mar. 1999.
[15] S. Cogollos, M. Brumos, V. E. Boria, C. Vicente, J. Gil, B. Gimeno, and M. Guglielmi, “A systematic design procedure of classical dual-mode circular waveguide filters using an equivalent distributed model,” *IEEE Trans. Microw. Theory Techn.*, vol. 60, no. 4, pp. 1006–1017, Apr. 2012.
[16] J. R. Montejo-Garai and J. Zapata, “Full-wave design and realization of multicoupled dual-mode circular waveguide filters,” *IEEE Trans. Microw. Theory Techn.*, vol. 43, no. 6, pp. 1290–1297, Jun. 1995.
[17] F. Arndt, R. Beyer, J. M. Reiter, T. Sieverding, and T. Wolf, “Automated design of waveguide components using hybrid mode-matching/numerical EM-building blocks in optimization-oriented CAD frameworks—State-of-the-art and recent advances,” *IEEE Trans. Microw. Theory Techn.*, vol. 45, no. 5, pp. 747–760, May 1997.
[18] M. Bekheit and S. Amari, “A direct design technique for dual-mode inline microwave bandpass filters,” *IEEE Trans. Microw. Theory Techn.*, vol. 57, no. 9, pp. 2193–2202, Sep. 2009.
[19] H. Hu and K.-L. Wu, “An automated design technique for asynchronously tuned circular waveguide dual-mode filters,” in *Proc. Asia–Pacific Microw. Conf.*, Yokohama, Japan, 2010, pp. 1970–1973.
[20] R. J. Cameron, C. M. Kudsia, and R. R. Mansour, *Microwave Filters for Communication Systems*. Hoboken, NJ: Wiley, 2007.
[21] R. Levy, “A generalized design technique for practical distributed reciprocal ladder networks,” *IEEE Trans. Microw. Theory Techn.*, vol. MTT-21, no. 8, pp. 519–526, Aug. 1973.
[22] G. L. Matthaei, L. Young, and E. M. T. Jones, *Microwave Filters, Impedance-Matching Networks and Coupling Structures*. New York: McGraw-Hill, 1964.
[23] μWave Wizard. ver. 7.7, Mician GmbH, Bremen, Germany, 2011.

Hai Hu (S'10) received the B.Sc. degree from Nanjing University, Nanjing, China, in 2004, the M.Phil. degree from The Chinese University of Hong Kong, Shatin, Hong Kong, in 2006, both in electronic engineering, and is currently working toward the Ph.D. degree at The Chinese University of Hong Kong.

From 2006 to 2010, he was a Research Assistant with the Department of Electronic Engineering, The Chinese University of Hong Kong, where he was involved with the numerical modeling of low-temperature co-fired ceramic (LTCC) layouts and passive integrated circuit components, automatic design of dual-mode waveguide filters, and manifold multiplexers for payload systems. His research interests include nonplanar filters, such as dielectric filters and compact multimode filter design and application for next-generation wireless base station systems, analytical CAT techniques, computational EM algorithms for modeling of waveguide structures, and frequency- and time-domain numerical modeling and analysis of multilayered high-speed RF circuits.

Mr. Hu was the recipient of the 2012 Asia–Pacific Microwave Conference Prize.

Ke-Li Wu (M'90–SM'96–F'11) received the B.S. and M.Eng. degrees from the Nanjing University of Science and Technology, Nanjing, China, in 1982 and 1985, respectively, and the Ph.D. degree from Laval University, Quebec, QC, Canada, in 1989.

From 1989 to 1993, he was with the Communications Research Laboratory, McMaster University, as a Research Engineer and a Group Manager. In March 1993, he joined the Corporate Research and Development Division, COM DEV International, the largest Canadian space equipment manufacturer, where he was a Principal Member of Technical Staff. Since October 1999, he has been with The Chinese University of Hong Kong, Shatin, Hong Kong, where he is currently a Professor and the Director of the Radiaofrequency Radiation Research Laboratory (R3L). He has authored or coauthored numerous publications in the areas of EM modeling and microwave passive components, microwave filters and antenna engineering. His current research interests include partial element equivalent circuit (PEEC) and derived physically expressive circuit (DPEC) EM modeling of high-speed circuits, RF and microwave passive circuits and systems, synthesis theory and practices of microwave filters, antennas for wireless terminals, LTCC-based multichip modules (MCMs), and RF identification (RFID) technologies. His research group is the main workforce in various active RFID research and applications in Hong Kong.

Prof. Wu is a member of the IEEE MTT-8 Subcommittee (Filters and Passive Components). He is a Technical Program Committee (TPC) member for many prestigious international conferences including the IEEE Microwave Theory and Techniques Society (IEEE MTT-S) International Microwave Symposium (IMS). He was an associate editor for the IEEE TRANSACTIONS ON MICROWAVE THEORY AND TECHNIQUES (2006–2009). He was the recipient of the 1998 COM DEV International Achievement Award for the development of exact EM design software of microwave filters and multiplexers, 2008 and 2012 Asia–Pacific Microwave Conference Prize.